국가기상위성센터
National Meteorological Satellite Center

Improved retrieval of sea ice surface properties from satellite passive-microwave observations

Sungwook Hong

NMSC/KMA

4th Asia/Oceania Meteorological Satellite Users' Conference, 9-11 October, Melbourne, Australia ♪

Outline

Introduction

- Sea ice is one of the most important variables in the global climate system, and in under standing the surface energy budget, fresh-water, and global temperature.

- Sea ice melting impacts on Ocean circulation, Melting of the Greenland Ice Sheet, Changes of animals, in vegetation, sea floor methane(Greenhouse gas), territorial claims (resources development, new shipping routes, sovereign rights)

\<http://nsidc.org/icelights/crash-course/arctic-sea-ice/ >

\<earthobservatory.nasa.gov\>
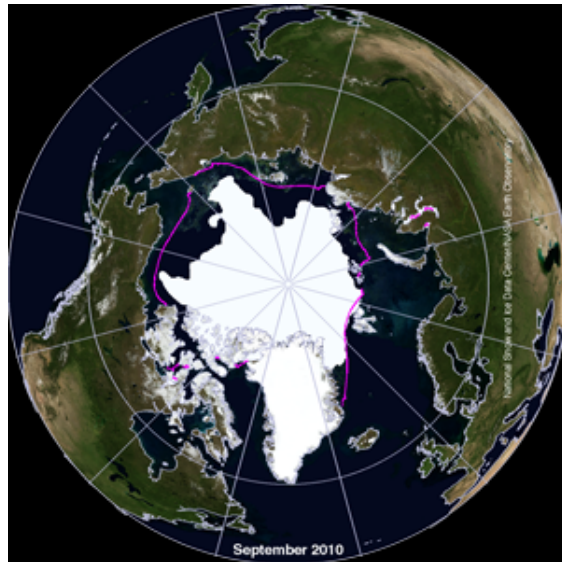
◆ **Sea ice extent was a minimum in Sept. 2007.**
◆ This research is in review.

Introduction

- Arctic shortcut in the Northern Sea
  - China (Aug. 21 2013)
    : Sailing a container-transporting vessel along
     the Northern Sea Route
  - Korea and Japan
    : Shipping oil products through the Arctic's melting
     ice along the Northern Sea Route.

- Arctic council
  - Member states
   : Canada, Finland, Iceland, Norway, Russia,
    Sweden, United States,
    Denmark; representing also the dependencies of
     Greenland and Faroe Islands
  - Permanent observer states
   : China, France, Germany, India, Italy, Japan,
    South Korea, Netherlands, Poland, Singapore,
    Spain, United Kingdom

China's New Shipping Frontier
How the new Northern Sea route compares
to the traditional Suez Canal route

NORTHERN SEA ROUTE
Travel time
35 days
Dangers
Icebergs
Travel window
July to November
Container-carrying vessels
**One this year**

SUEZ CANAL ROUTE
Travel time
48 days
Dangers
**Access to Suez Canal under
question with upheaval in Egypt**
Travel window
Year-round
Container-carrying vessels
17,000 last year
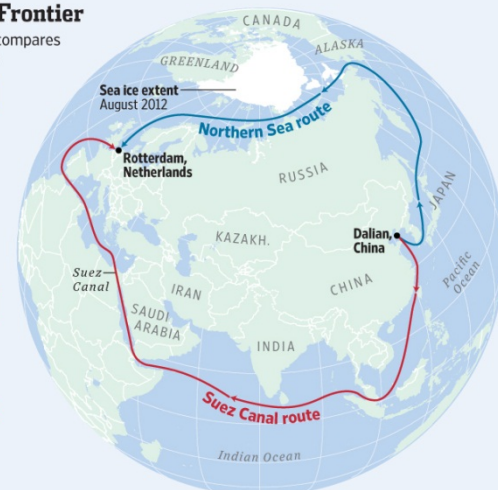
Sources: Northern Sea Route Information Office; National Snow and Ice Data Center; Cosco; Lloyd's List   The Wall Street Journal

http://online.wsj.com/article/SB10001424127887324619504579026031203525734.htm
l#project%3DARCTICSHIP%26articleTabs%3Dinteractive♪

Introduction
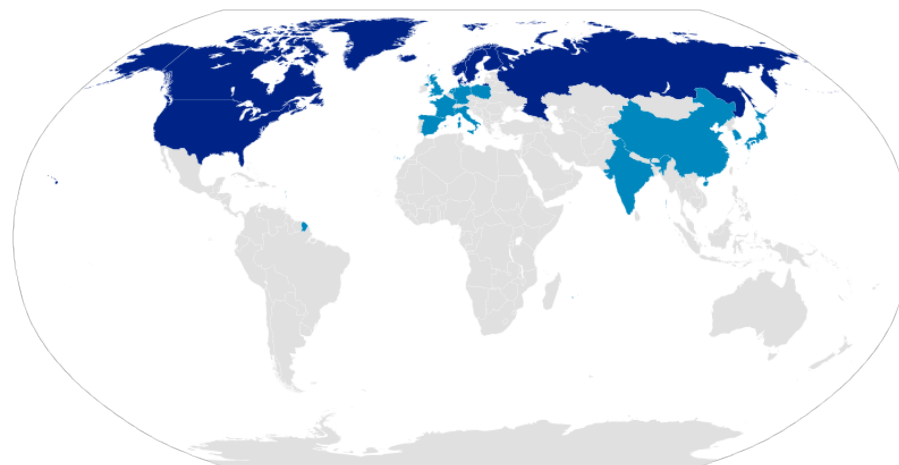
- Microwave satellite remote sensing is useful to monitor the change of sea ice because a large contrast in emissivity (or reflectivity) exists between sea ice and water.


AQUA/AMSR-E sensor♪

Table 2.1 – AMSR-E performance characteristics

CENTER FREQUENCIES (GHz)	6.925	10.65	18.7	23.8	36.5	89.0
BANDWIDTH (MHz)	350	100	200	400	1000	3000
SENSITIVITY (K)	0.3	0.6	0.6	0.6	0.6	1.1
MEAN SPATIAL RESOLUTION (km)	56	38	21	24	12	5.4
IFOV (km x km)	74 x 43	51 x 30	27 x 16	31 x 18	14 x 8	6 x 4
SAMPLING RATE (km x km)	10 x 10	10 x 10	10 x 10	10 x 10	10 x 10	5 x 5
INTEGRATION TIME (MSEC)	2.6	2.6	2.6	2.6	2.6	1.3
MAIN BEAM EFFICIENCY (%)	95.3	95.0	96.3	96.4	95.3	96.0
BEAMWIDTH (degrees)	2.2	1.4	0.8	0.9	0.4	0.18

Introduction

- Sea ice concentration is used in characterizing the spatial sea ice cover and extent and in the long-term trend analyses and process studies (Bjørgo et al. 1997; Cavalieri et al. 1997; Parkinson et al. 1999; Zwally et al. 2002)
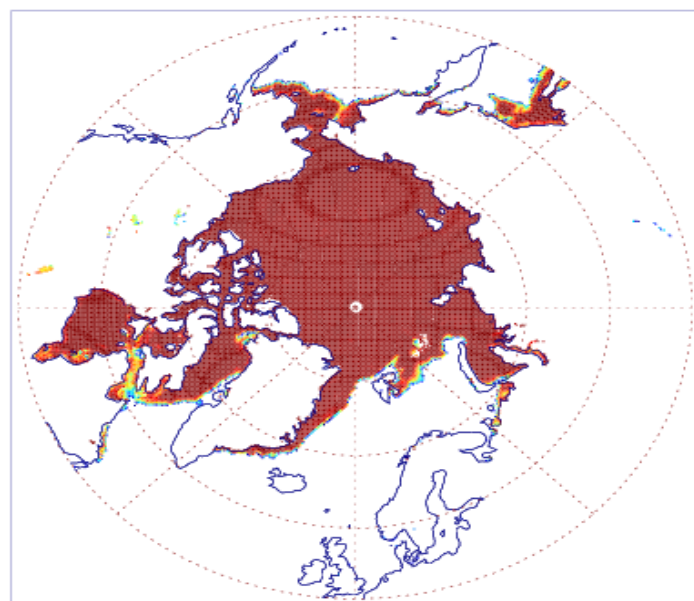
Sea ice concentration (%)

15.0   32.0   49.0   66.0   83.0   100.0

<Jan. 1 2007, Artic region >

Sea ice concentration (%)

15.0   32.0   49.0   66.0   83.0   100.0

<Jan. 1 2007, Antarctic region>

Introduction
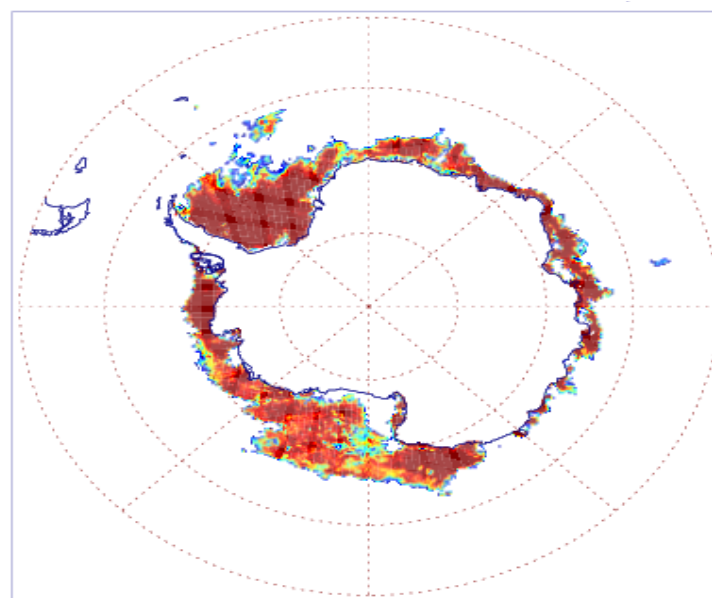
- Satellite microwave radiometer measure the energy emitted from the ocean surface.
  - The intensity of polarized radiation can be observed by microwave sensor depends on the **sea surface emissivity (or reflectivity)** .

- In this research, we investigate the following surface properties of sea ice:
  1. Small-scale surface roughness
  2. Refractive index of sea ice

- We propose an alternative approach for retrieving the sea ice properties using
  1. Hong approximation (Hong, 2009, J. Appl. Rem. Sens.)
  2. ASH(Azzam-Sohn-Hong) approximation (Hong, 2013, IEEE Geosci. Rem. Sens. Lett.)

The objective of this study is to improve retrieval of sea ice surface properties
from satellite passive-microwave observations

Theoretical Background

- **Fresnel equation**

$$R_{\mathrm{v}} = \left| \frac{\cos\theta - \sqrt{\hat{n}^2 - \sin^2\theta}}{\cos\theta + \sqrt{\hat{n}^2 - \sin^2\theta}} \right|^2 \quad \text{and} \quad R_{\mathrm{h}} = \left| \frac{\hat{n}^2 \cos\theta - \sqrt{\hat{n}^2 - \sin^2\theta}}{\hat{n}^2 \cos\theta + \sqrt{\hat{n}^2 - \sin^2\theta}} \right|^2$$

where θ is the view angle, $\hat{n} = n + ik$ ($i = \sqrt{-1}$) is the complex refractive index of the material and n and k are the real and imaginary parts of the refractive indices, respectively.

Augustin Fresnel
(1788-1827)
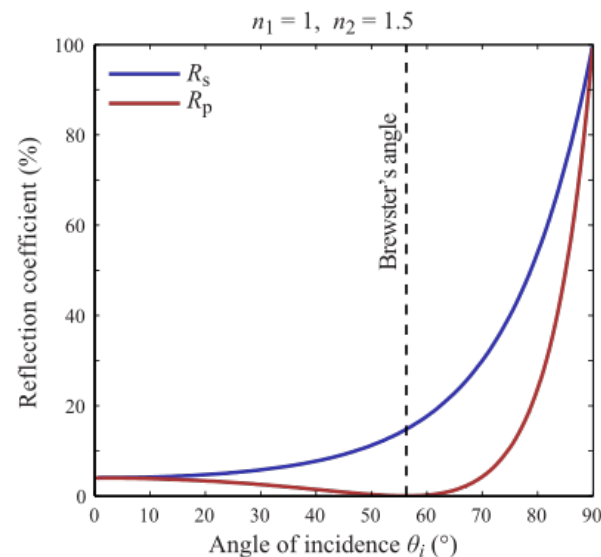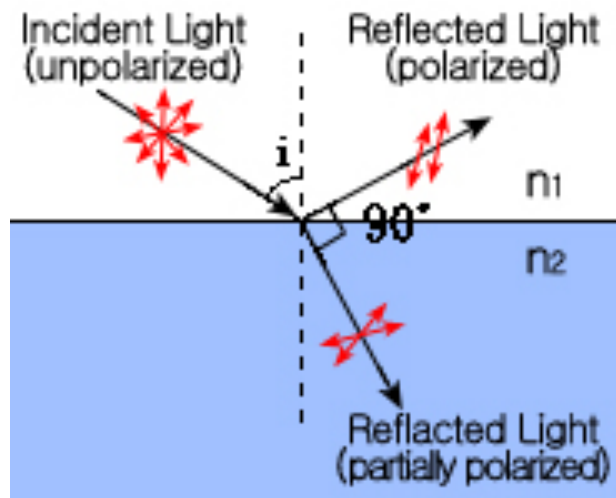
▪ **Questions**

   (1) Is there any relationship between polarized reflectivities if the refractive index is unknown?

   (2) How can we estimate the refractive index of a material?

  * We measure the reflectivities in a real world

  * Refractive index is a complex number

Theoretical Background

- **Fresnel equation**

$$R_v = \left| \frac{\cos\theta - \sqrt{\hat{n}^2 - \sin^2\theta}}{\cos\theta + \sqrt{\hat{n}^2 - \sin^2\theta}} \right|^2 \quad \text{and} \quad R_h = \left| \frac{\hat{n}^2\cos\theta - \sqrt{\hat{n}^2 - \sin^2\theta}}{\hat{n}^2\cos\theta + \sqrt{\hat{n}^2 - \sin^2\theta}} \right|^2$$

- Constraints:

(1) Two non-linear equations (← Fresnel equation)

(2) Three unknown variables (angle, real and imaginary parts of the refractive index) $\tilde{n} = n + i\kappa.$

➔ Difficult problem to be solved !

➔ Therefore, I tried to find a relationship between two polarizations irrespective of refractive index

Theoretical Background

- **Hong approximation** (Hong, 2009)
- **The generalized Fresnel equation** (Tousey, 1935)

$$R_V = \frac{(A_+ - \cos\theta)^2 + A_-^2}{(A_+ + \cos\theta)^2 + A_-^2} \quad \text{and} \quad R_H = R_V \times \frac{(A_+ - \sin\theta\tan\theta)^2 + A_-^2}{(A_+ + \sin\theta\tan\theta)^2 + A_-^2},$$

$$\text{with} \quad A_\pm^2 = [\sqrt{(n^2 - K^2 - \sin^2\theta)^2 + 4n^2 k^2} \pm (n^2 - K^2 - \sin^2\theta)]/2.,$$

- From taking the first term in the Taylor series for natural logarithmic ratio of ln R_H/ln R_V, we can obtain the Hong approximation as follows (Hong, 2009):

$$\frac{\ln R_H}{\ln R_V} = 1 + \frac{\ln(1+X_3) - \ln(1+X_4)}{\ln(1+X_1) - \ln(1+X_2)}$$

with $X_1 = (Q - \cos\theta)^2 + P^2 - 1$, $\qquad X_2 = (Q + \cos\theta)^2 + P^2 - 1$,

$X_3 = (Q - \sin\theta\tan\theta)^2 + P^2 - 1$, and $X_4 = (Q + \sin\theta\tan\theta)^2 + P^2 - 1$.

After taking the first term in the Taylor series for natural logarithm ($\ln(1+x) = x - x^2/2 + x^3/3 + O(x^4)$) without the strict constraints ($-1 < x \leq 1$), the approximation of Eq. (2) is as follows:

$$\frac{\ln R_H}{\ln R_V} \approx 1 + \frac{X_3 - X_4}{X_1 - X_2} = 1 + \frac{\sin\theta \cdot \tan\theta}{\cos\theta} = \frac{1}{\cos^2\theta}$$

$$\boxed{R_H = R_V^{1/\cos^2\theta}}$$

- **Hong approximation** (Hong, 2009)
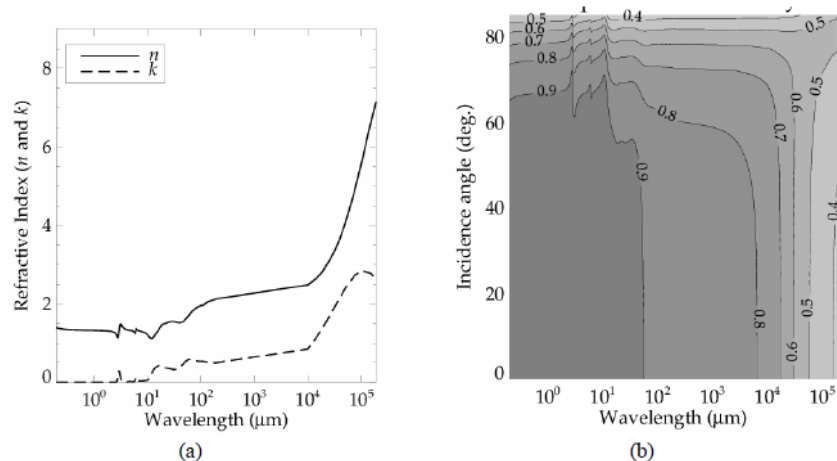
Fig. 1. (a) Refractive index of water and (b) unpolarized emissivity. The same wavelength range is used as that shown in Figure 1. The unpolarized emissivity is calculated using the Fresnel equations and the refractive index of water for various incidence angles.
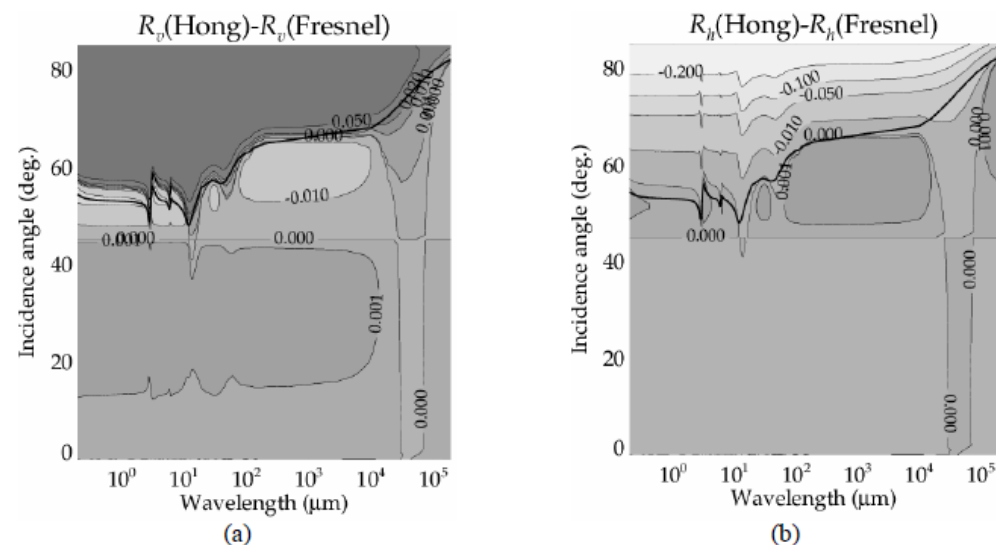

Fig. 2. Validation of the Hong approximation. (a) R_V (Fresnel)$-$ R_V (Hong) and (b) R_H (Fresnel) $-$ R_H (Hong) are shown. The wavelength range is the same as that shown in Fig. 1.

1. Decomposition of unpolarization

(1) Hong approximation

$$R_H = R_V^{1/\cos^2\theta}$$

(2) Unpolarized reflectivity

$$R = \frac{R_v + R_h}{2},$$

Hong graph: $R_h = R_v^{(1/\cos\theta)^3}$, $R_h = 2(1-E) - R_v$

Bias: R_v — R_v(Simulation)$-R_v$(Fresnel) vs Wavelength (µm)

View:10, View:20, View:30, View:40, View:50, View:60

Bias: R_h — R_h(Simulation)$-R_h$(Fresnel) vs Wavelength (µm)

(a)　　(b)

Hong,2010 (Int. J. Rem. Sens.)

Applications of Hong approximation
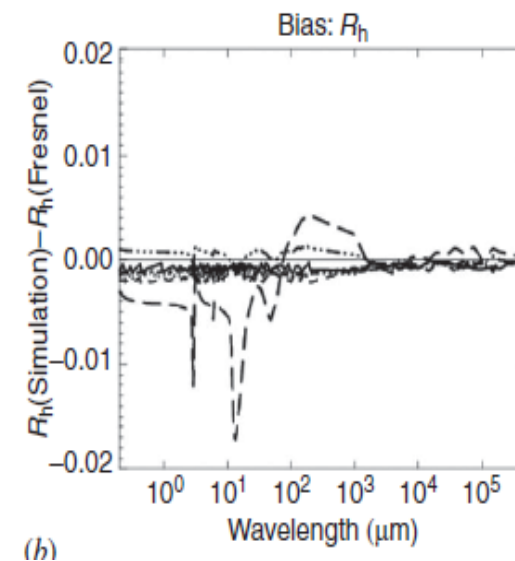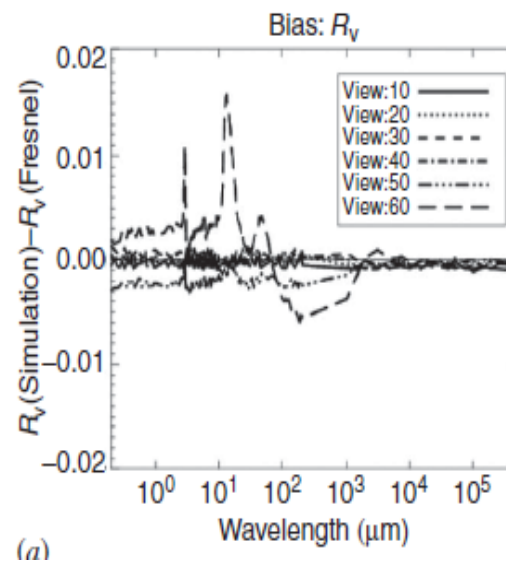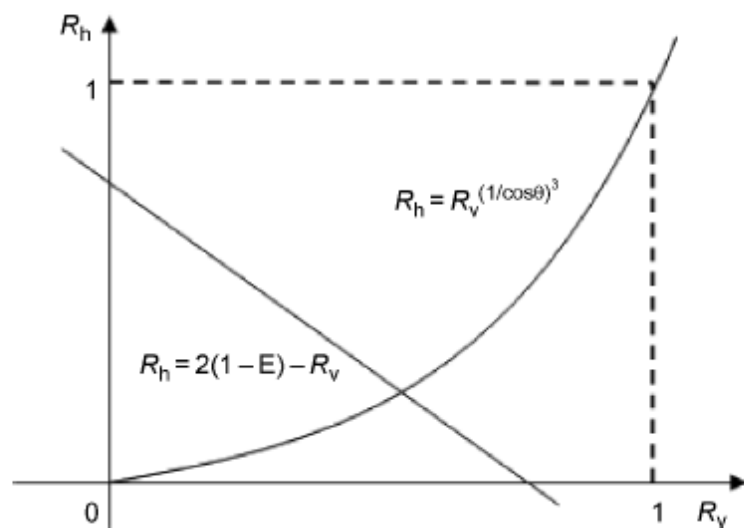
2. Refractive Index

: Derived a theoretical relationship between polarized reflectivites
: Provide how to estimate the refractive index (intrinsic property of materials)

$$R_{\mathrm{v}} = \left| \frac{\cos\theta - \sqrt{\hat{n}^2 - \sin^2\theta}}{\cos\theta + \sqrt{\hat{n}^2 - \sin^2\theta}} \right|^2 \quad \text{and} \quad R_{\mathrm{h}} = \left| \frac{\hat{n}^2\cos\theta - \sqrt{\hat{n}^2 - \sin^2\theta}}{\hat{n}^2\cos\theta + \sqrt{\hat{n}^2 - \sin^2\theta}} \right|^2,$$

Querry (1969)

$$n = \sqrt{\frac{A_+^2 - A_-^2 + \sin^2\theta + \sqrt{(A_+^2 + A_-^2 - \sin^2\theta)^2 + 4A_-^2 A_+^2}}{2}} \quad \text{and} \quad K = \frac{A_- A_+}{n}, \qquad (9)$$

where $A_- = \sqrt{-A_+^2 - 2FA_+\cos\theta - \cos^2\theta}$, $\qquad A_+ = [(F-G)\sin\theta\cot2\theta]/[GF + (1-F^2)\cos^2\theta - 1]$,

$F = (R_V + 1)/(R_V - 1)$, $\qquad$ and $\qquad G = (R_H + 1)/(R_H - 1)$.
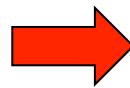
(Hong, 2009)
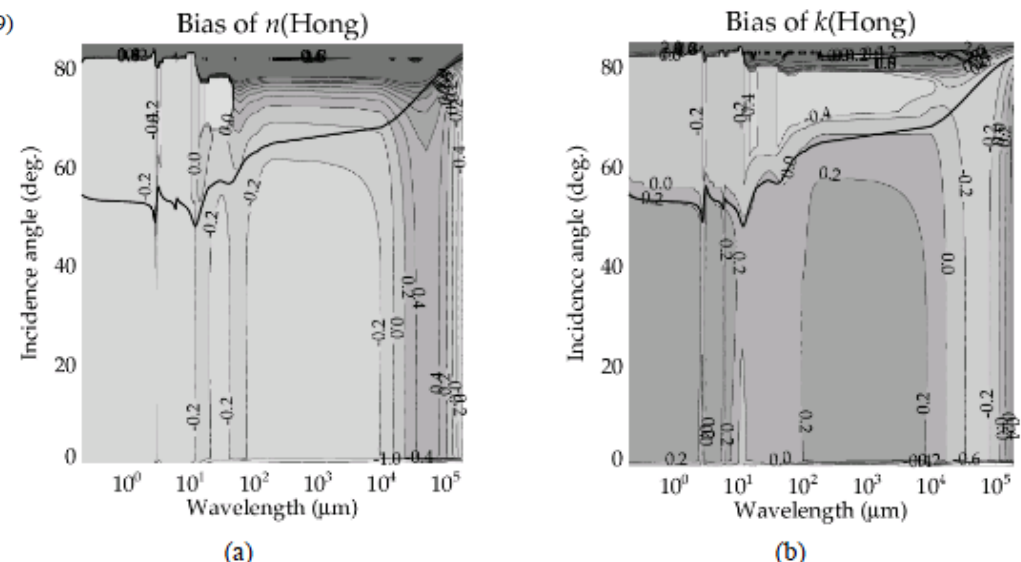
Fig. 4. Bias of the retrieved refractive index of water for (a) n and (b) K.

3. Surface Roughness

$$R_{R,V} \approx R_{S,V} \approx 0 \text{ and } R_{R,H} < R_{S,H} \qquad R_{S,H} = R_{S,V}^{\cos^2 \theta}$$

$$\sigma = \frac{\lambda}{4\pi \cos \theta} \cdot \sqrt{\ln \left(\frac{R_{R,V}^{\cos^2 \theta}}{R_{R,H}} \right)}$$

incident wave

scattering wave

rough

σ (cm)

0.00   0.03   0.05   0.08   0.10
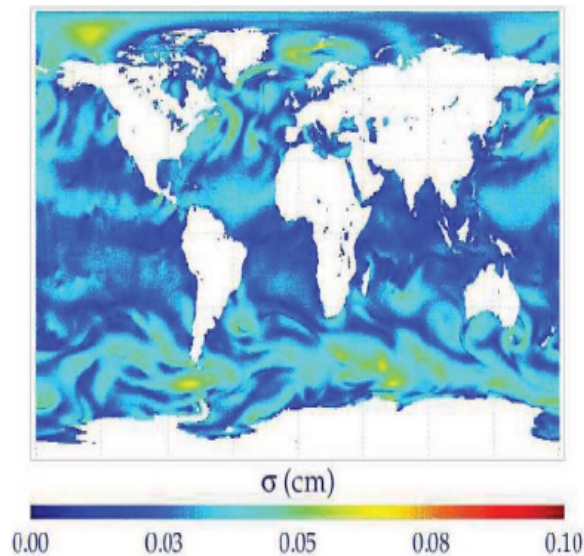
Figure 4. Sea surface roughness at SSM/I 19 GHz channel for 24 February 2009 (06 UTC).
FASTEM-2, Fresnel equations, equation (1), and GDAPS data of 24 February 2009 were used.
The small-scale surface roughness ranged from 0 to 0.07 cm in this case.

Hong, 2010 (Int. J. Rem. Sens.)

a   b

σ (cm)   σ (cm)
0.0   0.5   1.0   1.5   2.0   0.0   0.5   1.0   1.5   2.0

c   d

σ (cm)   σ (cm)
0.00   0.20   0.40   0.60   0.80   0.00   0.20   0.40   0.60   0.80
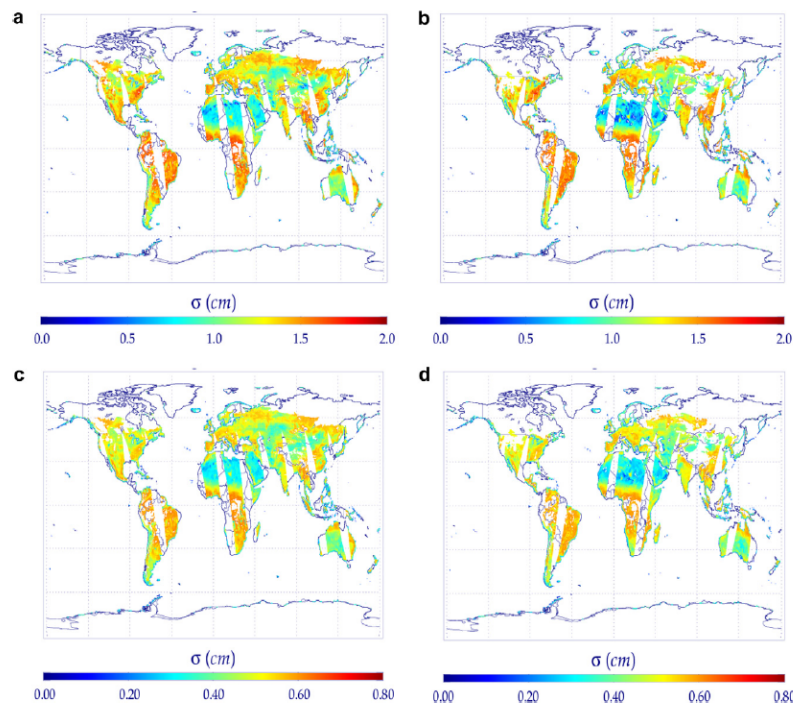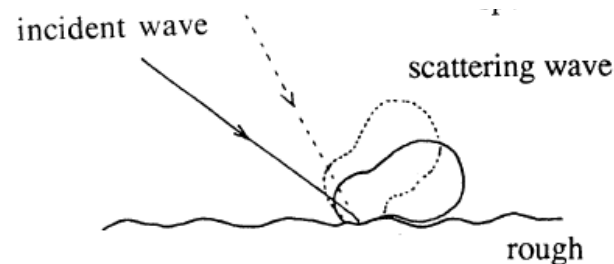
Fig. 5. Estimated σ using W–C model at AMSR-E (a) 6.9 GHz (ascending), (b) 6.9 GHz (descending), (c) 10 GHz (ascending), and (d) 10 GHz (descending). The σ is relatively low for the desert and bare soil regions, and relatively high for vegetation regions.

Hong, 2010 (J. Hydrol.)

Applications of Hong approximation
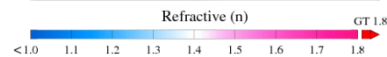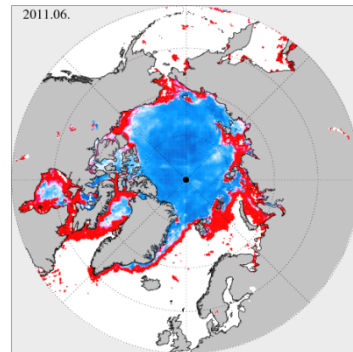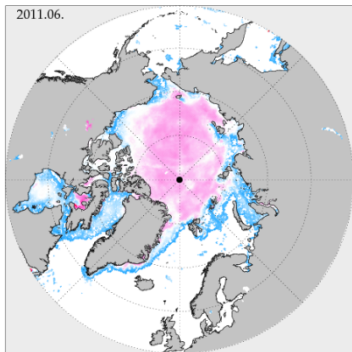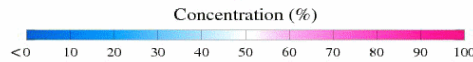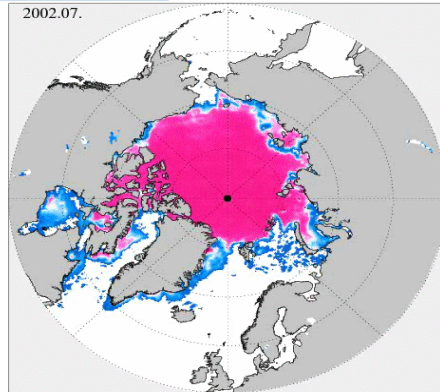
4. Sea ice

Concentration, Small-scale roughness and refractive in dex of sea ice surfaces (June. 2011) using AQUA/AMS R-E data♪

Hong, 2010 (Rem. Sens. Environ.)   **Hong and Shin, 2010 (J. Climate)**
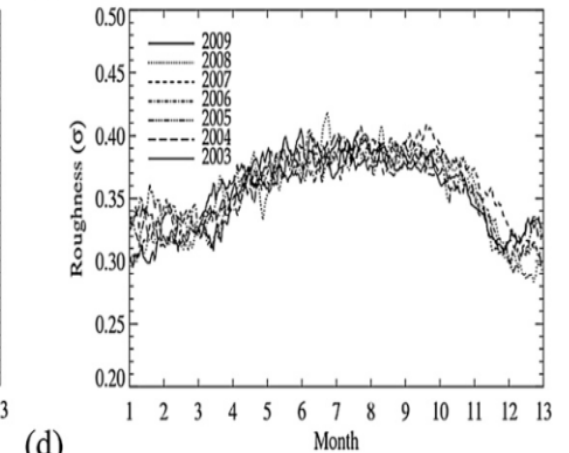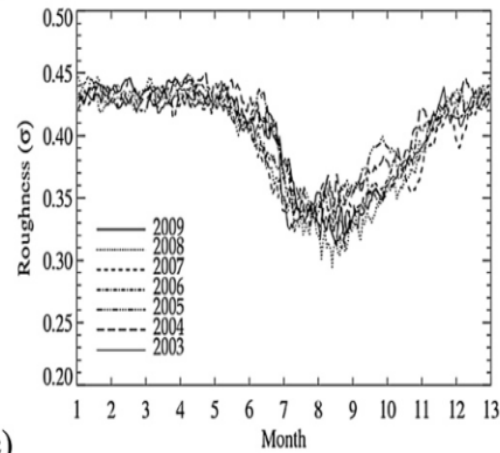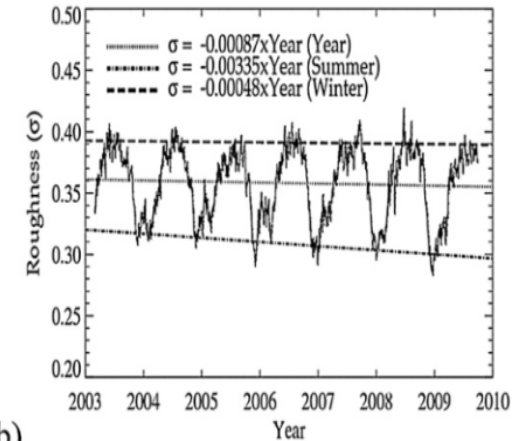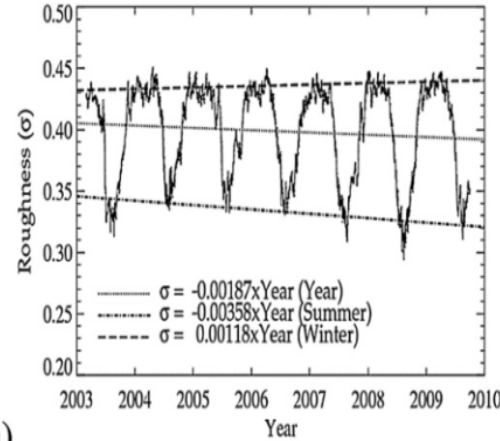
5. Soil moisture
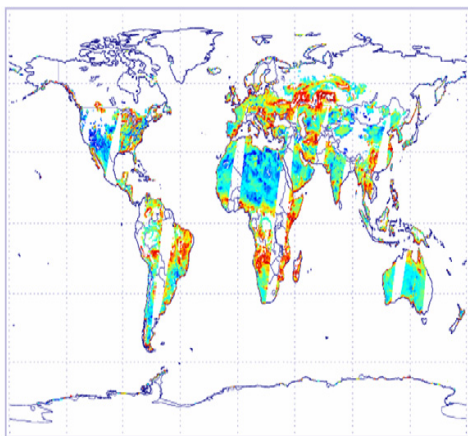
(a) Volumetric soil water content (g/cm3) using Hong's algorithm
(b) AMSR-E level 3 products.

Hong and Shin, 2011 (J. Hydrol.)

6. Wind speed

AMSR-2 6.9GHz wind

- **Hong and Shin (2013)**

Theoretical Background
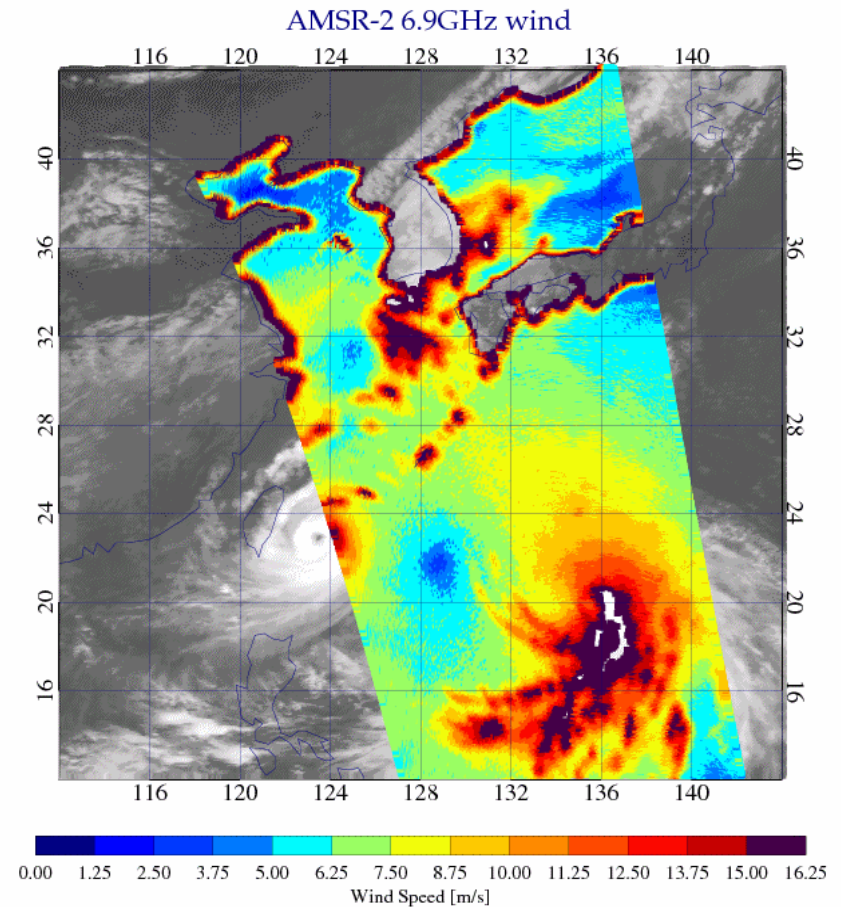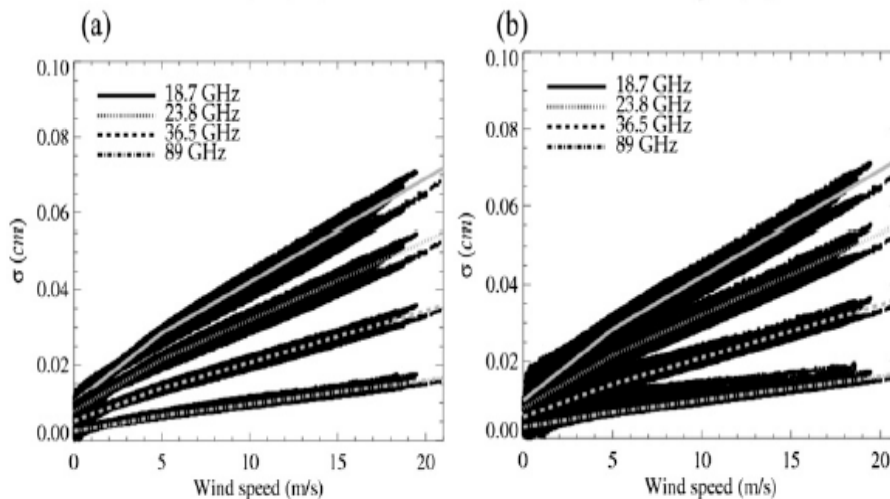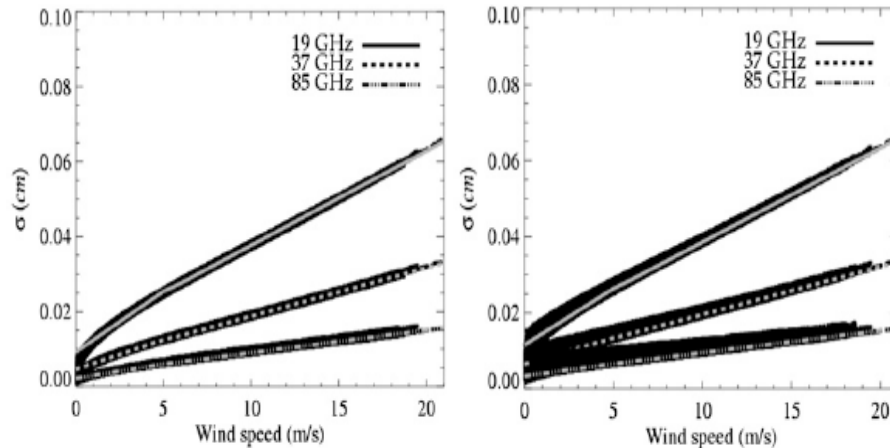
- **Direct relationship (Azzam relationship) (Hong, 2013 (IEEE GRSL)**

$$R_{S,H} = R_{S,V}$$
$$\times \frac{(\sqrt{R_{S,V}} - \cos 2\theta)^2 + 2(\sqrt{R_{S,V}} - \text{Re}(\hat{r}_V) \cdot \cos 2\theta)}{(1 - \sqrt{R_{S,V}} \cdot \cos 2\theta)^2 + 2(\sqrt{R_{S,V}} - \text{Re}(\hat{r}_V) \cdot \cos 2\theta)}$$

where $R_{S,V} = \text{Re}(\hat{r}_V)^2 + \text{Im}(\hat{r}_V)$ such that $\text{Re}(\hat{r}_V)$ and $\text{Im}(\hat{r}_V)$ are the real and imaginary parts of $\hat{r}_V$, respectively.

← **Azzam (1979, 1986)**

Starting from (1) by substituting $\hat{n}^2$ into (2) and using $\cos^2 \theta = (1 + \cos 2\theta)/2$, the following relationship between the complex Fresnel reflection coefficients has been obtained [27], [28]

$$\hat{r}_H = \hat{r}_V \cdot \frac{\hat{r}_V - \cos 2\theta}{1 - \hat{r}_V \cdot \cos 2\theta}.$$

- Weakness: it still needs *a priori* information

- In case of k ~ 0 (for example, dielectrics; For metals, k > n), Azzam relationship can be reduced to ASH (Azzam-Sohn-Hong) approximation as follows (Hong, 2013 (IEEE GRSL)):

$$R_{S,H} = R_{S,V} \cdot \frac{(\sqrt{R_{S,V}} + \cos 2\theta)^2}{(1 + \sqrt{R_{S,V}} \cdot \cos 2\theta)^2}$$

Method

- **Roughness effect on the surface emissivity**

  - Passive microwave emission is affected by ice surface roughness as a complex function of the frequency, polarization, sensor-surface geometry of the radiometer, and complex permittivity of the material bounded below by the rough surface (Kong et al., 1979; Grenfell and Lohanick, 1985; Grenfell, 1992; Barber et al.,

    1998; Grody, 2008)
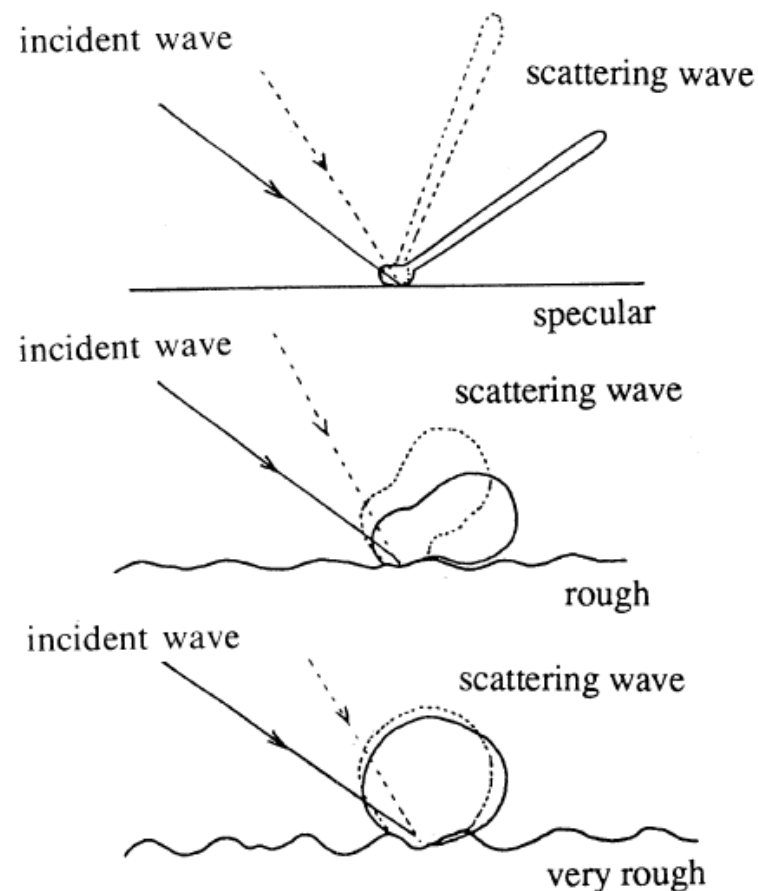
- **Scale vs. Wavelength**

  - Small-scale   (roughness < wavelength)

  - Large-scale (roughness > wavelength)

Method

■ **Roughness effect on the surface emissivity**

- A semiempirical model based on the incoherent approach is used for small-scale surface

roughness, which corresponds to identifying the height probability density function with a

Gaussian distribution of zero mean and variance as follows (Wu & Fung, 1972, Choudhury et

al., 1979):
$$R_R = R_S \cdot \exp\left[-\left(\frac{4\pi\sigma\cos\theta}{\lambda}\right)^2\right]$$

where R is the reflectivity, σ is the small-scale roughness height (Ulaby et al., 1982), λ is the wavelength, θ is the incidence angle. Subscripts R and S mean 'rough' and 'specular', respectively.

■ **Small scale roughness retrieval**

  - Hong approximation(Hong, 2009): $R_{S,H} \approx R\downarrow R,v\uparrow\sec2\theta$

  - ASH approximation (Hong, 2103): $R_{S,H} = R_{S,V} \cdot \dfrac{(\sqrt{R_{S,V}} + \cos2\theta)^2}{(1 + \sqrt{R_{S,V}} \cdot \cos2\theta)^2}.$
  - Estimate using the observed rough surface reflectivities near the Brewster angle (Hong, 2010
)

  Small scale Roughness: $\sigma \approx \lambda/4\pi\cos\theta \cdot \sqrt{\ln(R\downarrow R,v\uparrow\sec2\theta / R_{R,H})}$

Method

- **Surface refractive index**

  - Conversion rough surface reflectivity to specular surface reflectivity

  - AMSR-E TB & Ts

    → Rough surface reflectivity

    → Specular surface reflectivity

    → Inversion method to estimate surface refractive index

    Surface roughness

    $$\sigma \approx \frac{\lambda}{4\pi \cos\theta} \cdot \sqrt{\ln\left(\frac{R_{R,V}^{\sec^2\theta}}{R_{R,H}}\right)}$$

- **Retrieval of Surface refractive index** (Querry, 1969 (J. Opt. Soc. Am.))

$$n = \sqrt{\frac{A_+^2 - A_-^2 + \sin^2\theta + \sqrt{(A_+^2 + A_-^2 - \sin^2\theta)^2 + 4A_-^2 A_+^2}}{2}} \quad \text{and} \quad K = \frac{A_- A_+}{n},$$

where $A_- = \sqrt{-A_+^2 - 2FA_+\cos\theta - \cos^2\theta}$, $\quad A_+ = [(F-G)\sin\theta\cot 2\theta]/[GF + (1-F^2)\cos^2\theta - 1]$,

$F = (R_V + 1)/(R_V - 1)$, $\quad$ and $\quad G = (R_H + 1)/(R_H - 1)$.

Data and Procedure

- **Data**

  - AMSR-E level-3 data (25 km gridded data)

  - channels : 6.925, 10.65, 18.7, 23.8, 36.5, and 89.0 GHz

  - Jun. 2002 to Sep. 2011

- **Procedure**

```
┌─────────────────────────┐      ┌──────────────────────────────────────┐
│  AMSR-E observations     │ ───→ │ Rough Surface reflectivities at the   │
│                          │      │ AMSR-2 18.9, 23.8, 36,5 GHz           │
└─────────────────────────┘      └──────────────────────────────────────┘
                                                   ⇩
                                  ┌──────────────────────────────────────┐
                                  │          Surface Roughness            │
                                  └──────────────────────────────────────┘
                                                   ⇩
                                  ┌──────────────────────────────────────┐
                                  │        Surface refractive index       │
                                  └──────────────────────────────────────┘
                                                   ⇩
                                  ┌──────────────────────────────────────┐
                                  │              Analysis                 │
                                  └──────────────────────────────────────┘
```
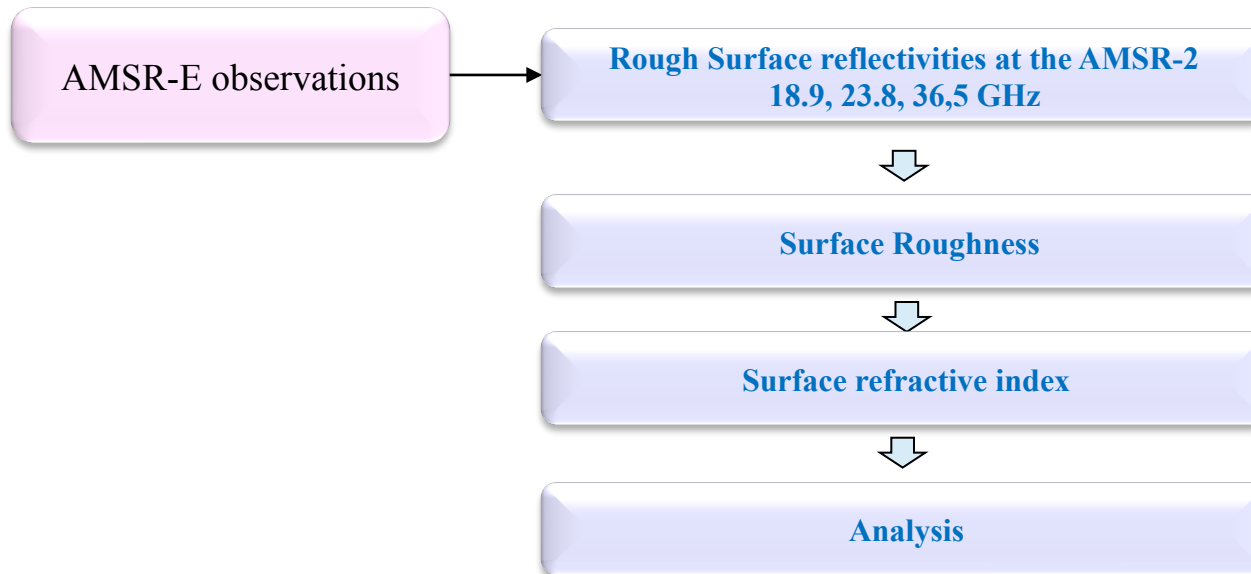
- **Surface temperature (Comiso et al. 2003)**

$$T_S = T_{B,V}(6.9)/[1 - R_{R,V}(6.9)]$$

where $R_{R,P}(6.9)$ is 0.02 for ice (Markus and Cavalieri, 2000) and 0.44 for ocean (Hwang and Barber, 2008)

At other frequencies such as 18.7 GHz, the $R_{R,P}$ of the sea ice surface is estimated for polarization (P =V or H) as follows:

$$R_{R,P}(18.7) = 1 - \frac{T_{B,P}(6.9)}{T_{B,P}(18.7)}[1 - R_{R,P}(6.9)]$$

Finally, the mixed surface reflectivity of the ice and water on the rough sea ice surface is described as follows (Nishio and Comiso, 2005):

$$R_{R,V} = R_{R,V,ice} + (R_{R,V,ice} - R_{R,V,water}) \cdot \left[1 - \frac{C_I}{100}\right]$$

where C_I is defined as the percentage of sea ice within the field of view of the sensor (Nishio and Comiso, 2005).

- Absolute difference in R_H between the Fresnel equation and the ASH and Hong approximations for (a) ice and (b) water. AMSR-E has an incidence angle of 55º.
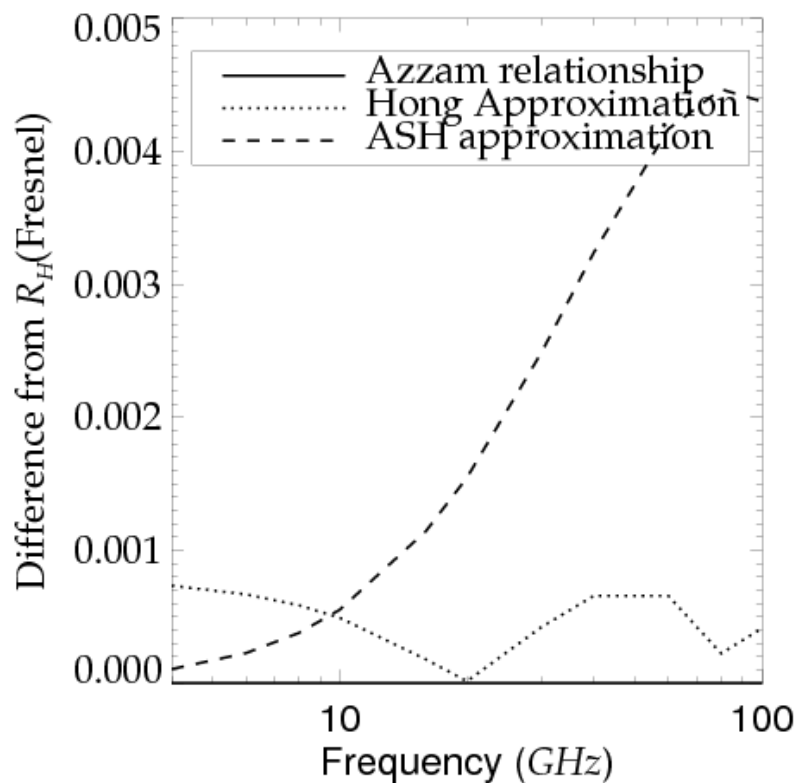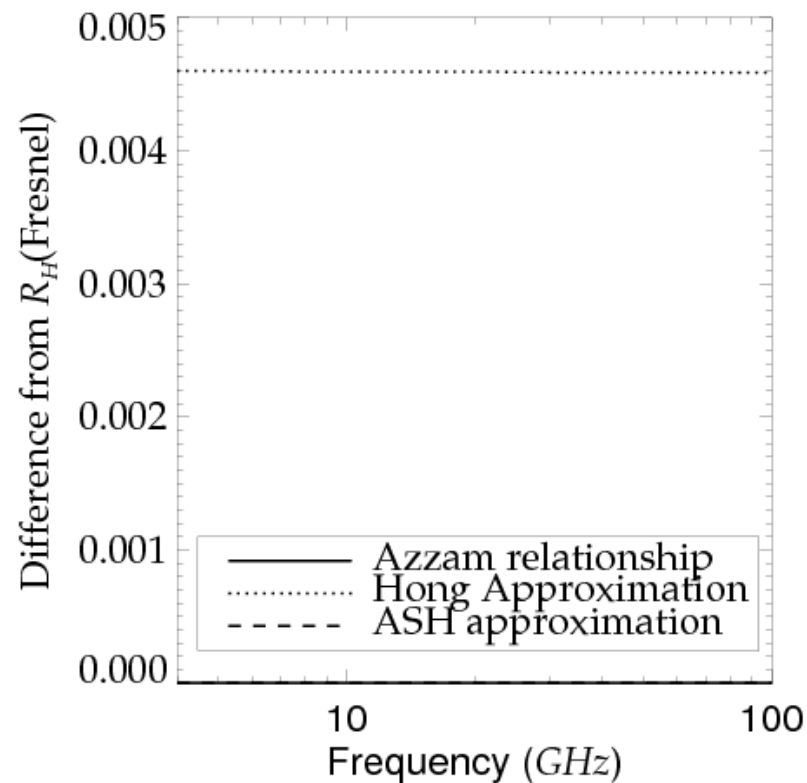

For water♪

For ice♪

- Small-scale surface roughness ϭ retrieved for the Arctic using the Hong approximation and the ASH approximations in the 18.7 GHz channel of AMSR-E.
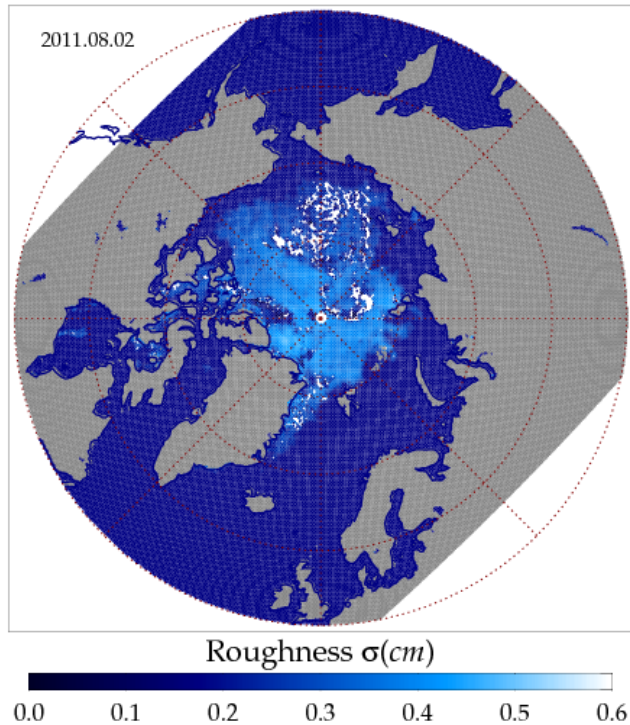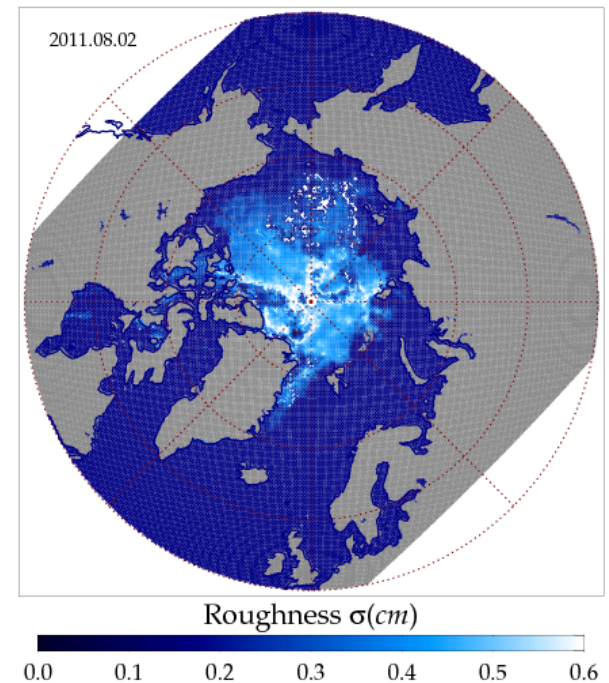

Hong approximation♪

ASH approximation♪

- The time series of ϭ from 2002 to 2011 show (c) the decreasing trend.

  The differences are relatively large in the melting seasons
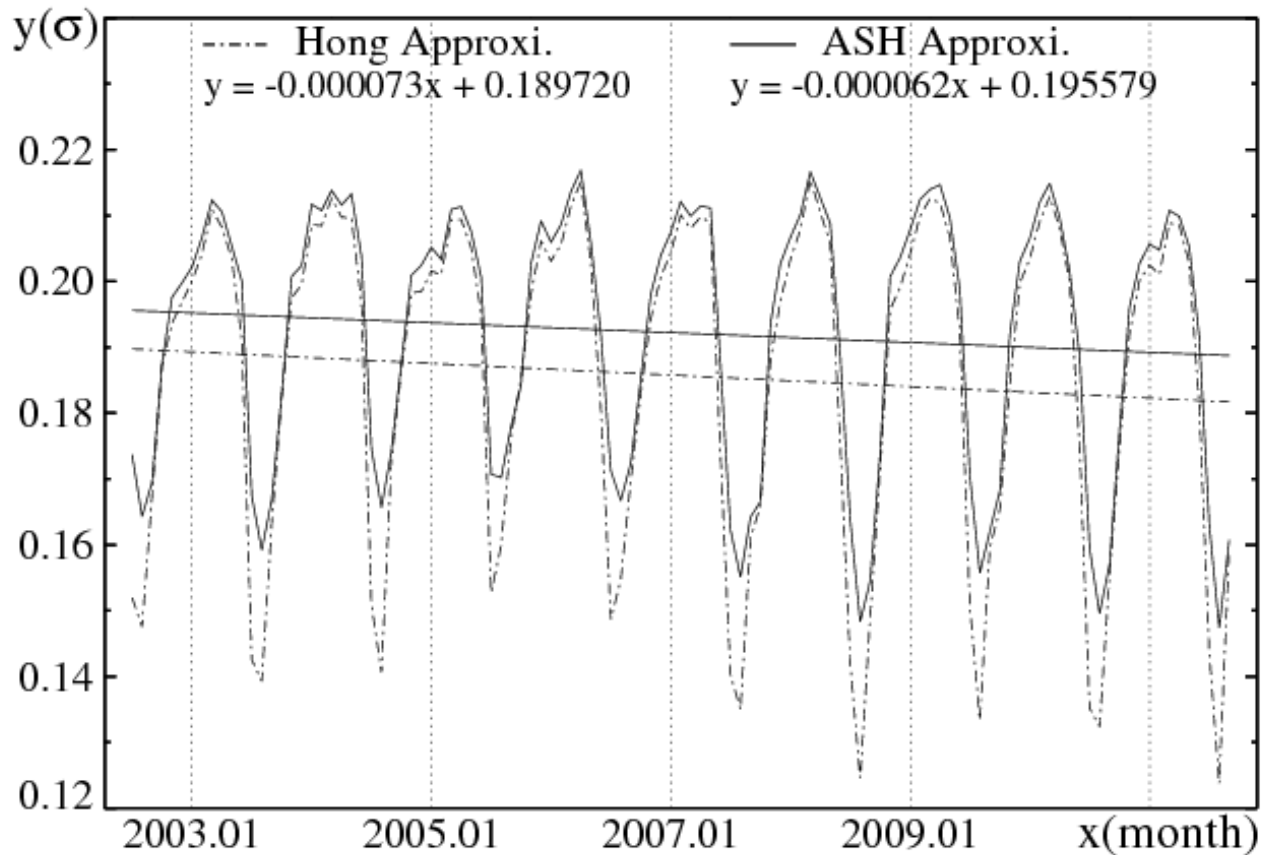
Results (Refractive index)

- Refractive index *n* retrieved for the Arctic using the Hong approximation and the ASH approximations in the 18.7 GHz channel of AMSR-E.

Hong approximation♪   ASH approximation♪

- The time series of n from 2002 to 2011 show the increasing trend. The sea ice surface is melting because n is closer to that of water.

Summary and Conclusion
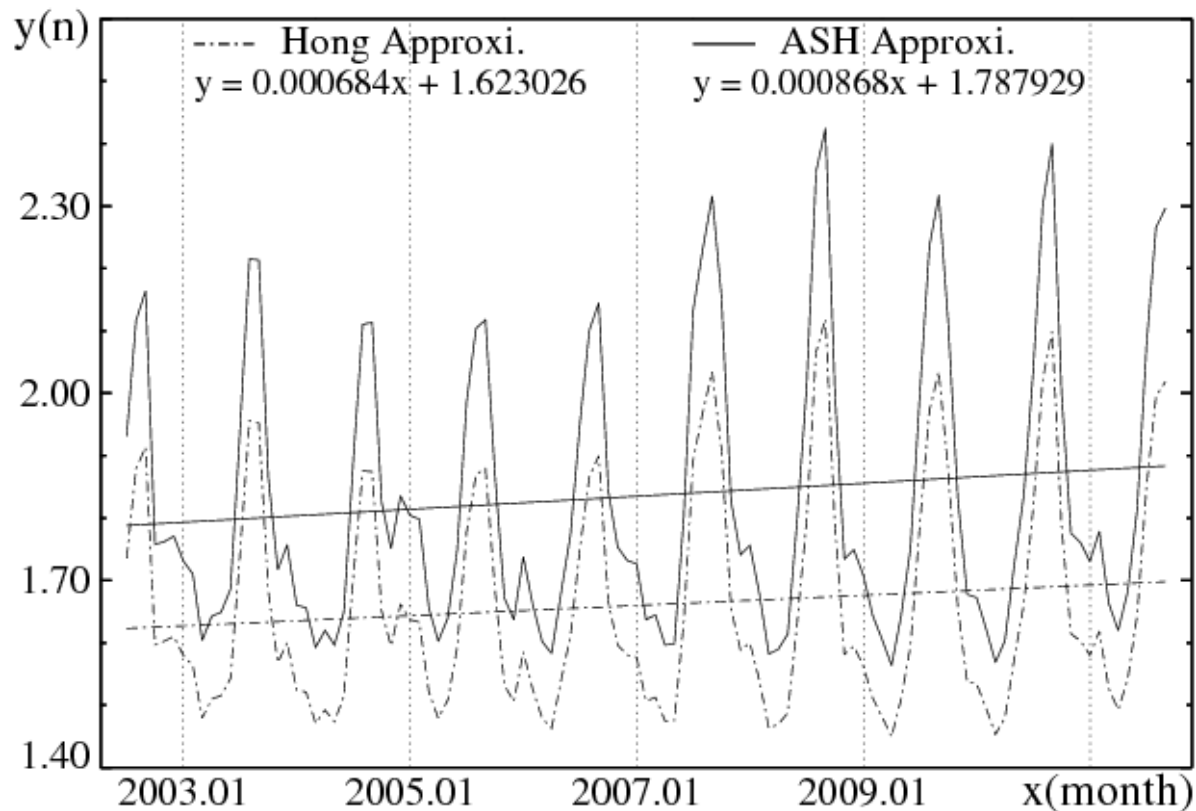
- The ASH and Hong approximations were applied to investigate the characteristics of the polar sea ice surface using the daily L3 25-km data of AMSR-E.

- The effective rough surface reflectivities were estimated for V and H polarizations.

- In turn, the surface roughness and refractive index were estimated using the ASH and Hong approximations.

- The ASH approximation produces a better result for sea ice than for water (Winter), while the Hong approximation is more effective for water than for sea ice in melting seasons (Summer).

- In conclusion, the combination of the ASH and Hong approximations is effective to estimate the small-scale roughness and refractive index for physical interpretations of sea ice melting due to climate change.

- This investigation supports the phenomenon of sea ice melting on the basis of the decreasing trend in the small-scale roughness and the increasing trend in the refractive index.

Thank you

Applications of Hong approximation

8. Oil spill detection

● Reflectivities
- Rv over oil : 0.07 ~ 0.1, Rh : ~ 0.04
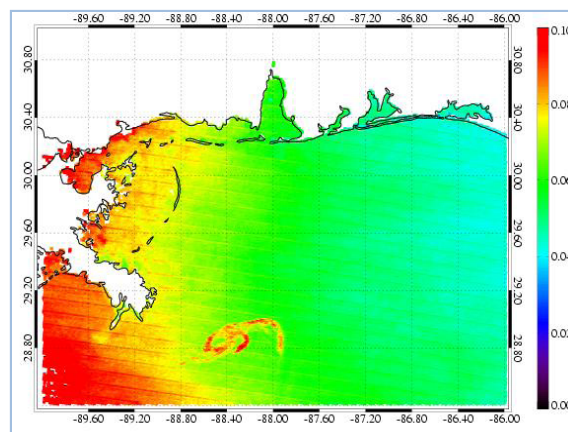
● Refractive index
- n : 1.25 ~ 1.4   (oil), 1.1 ~ 1.25 (sea-water)
- k : 0.45 ~ 0.5 (oil), 0.4   ~ 0.45 (water)
- n values : physical, while k values are not physical but effective

- **In review (2013)**
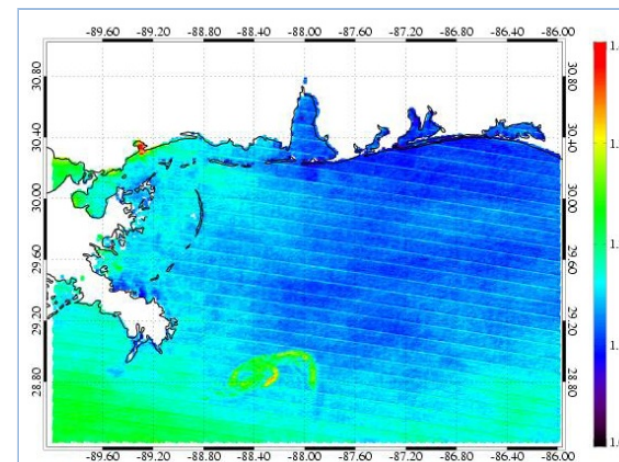
## 10. Flood monitoring
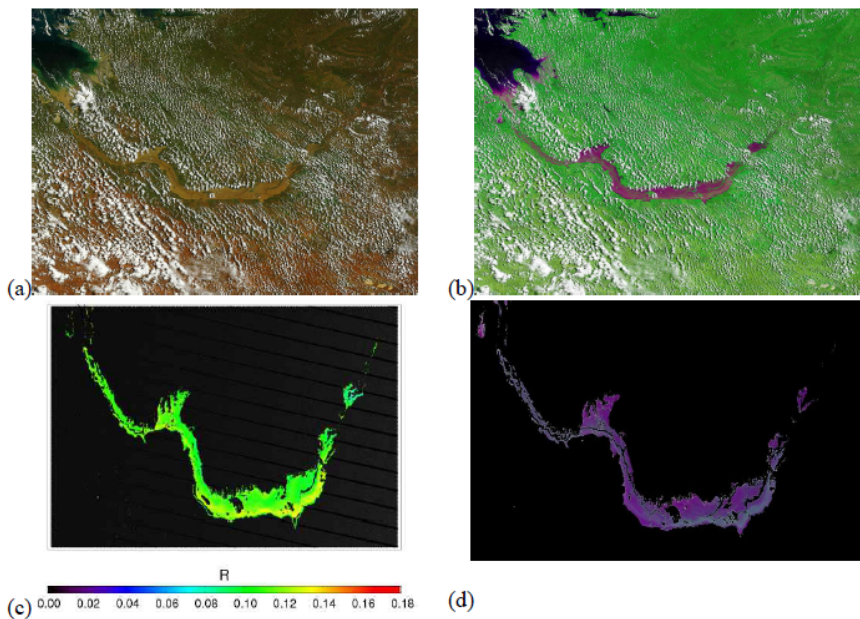
- In review
- a flooding along the Fitzroy river area of Western Australia on March 17, 2011
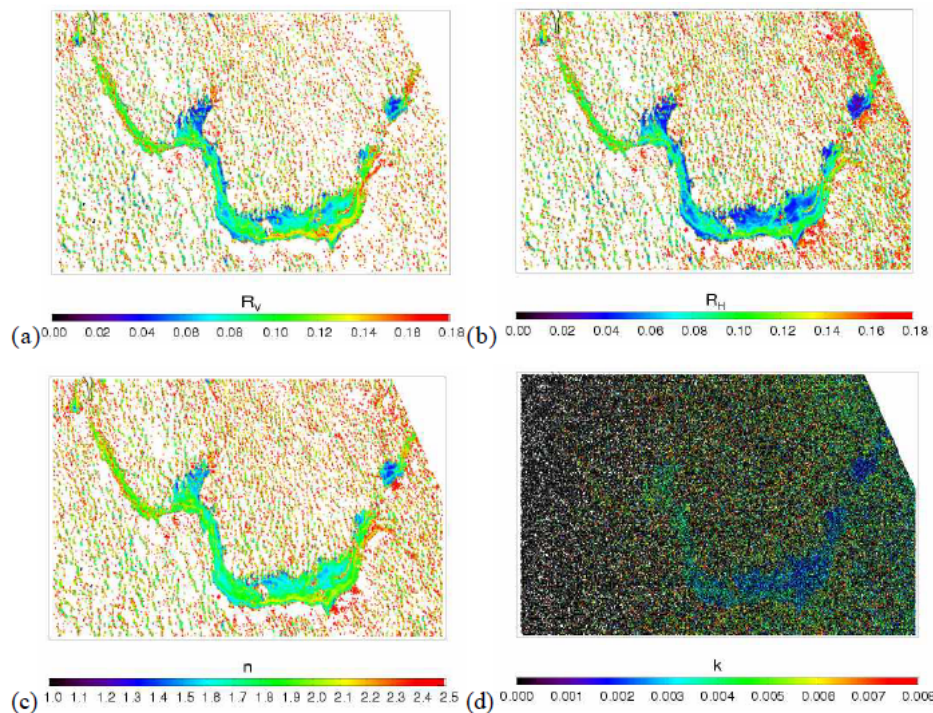
4. Asian dust

- Hong, 2009 (Atmos. Environ.)
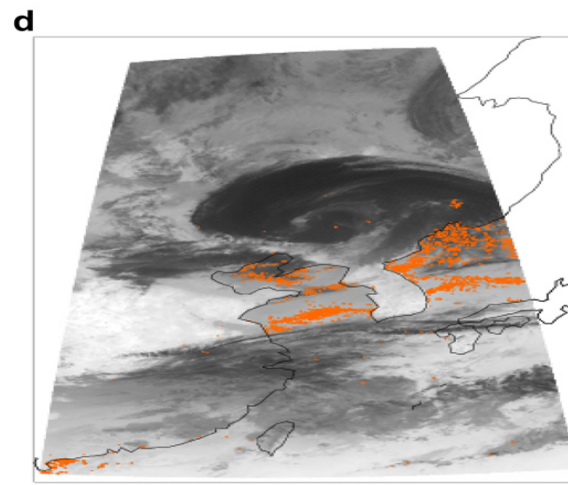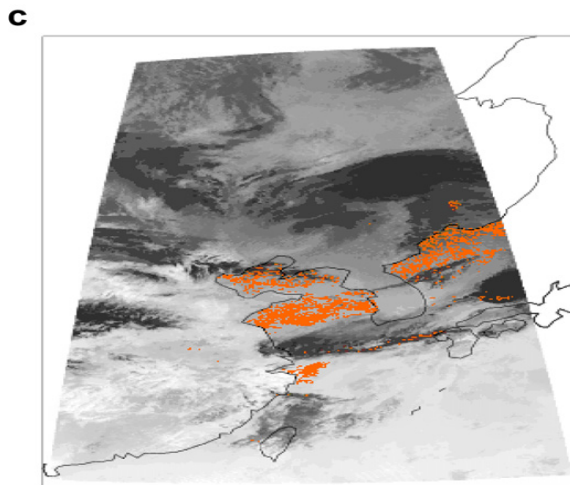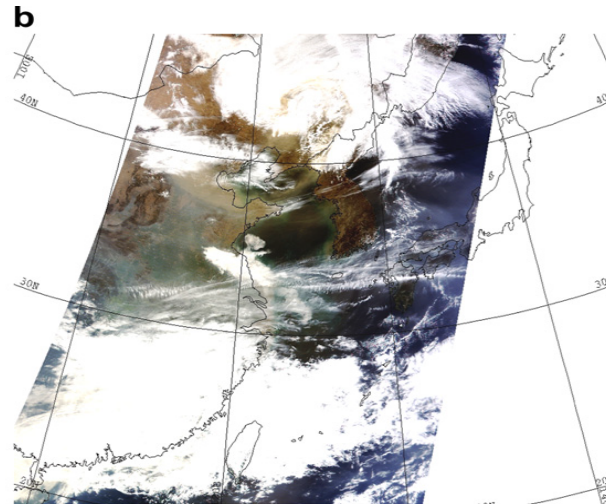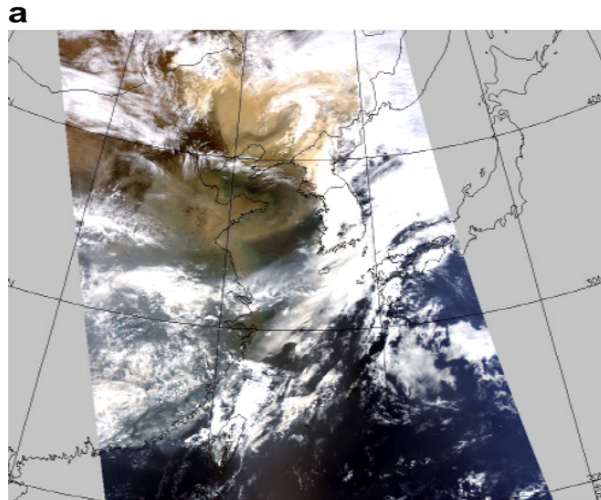
Applications of Hong approximation

## 3. Emissivity model (Radiative transfer model)
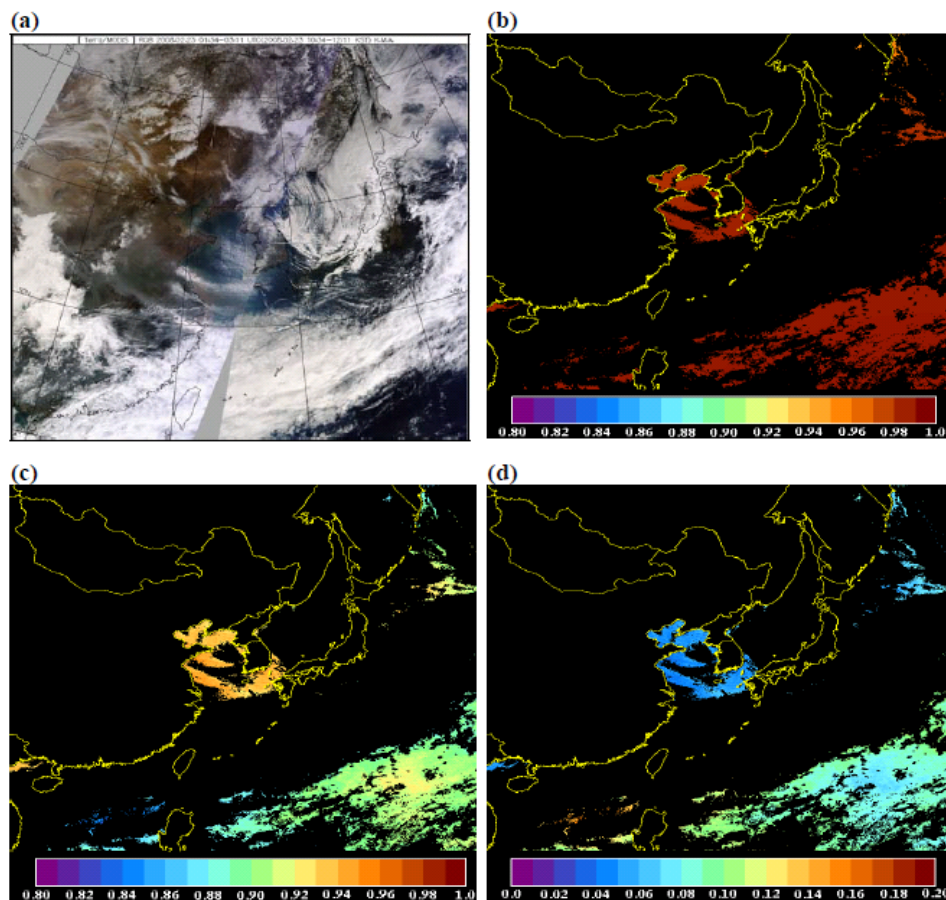
FIG. 3. MODIS RGB composite image and emissivities for the NW Pacific region. (a) MODIS RGB image, (b) IE, (c) PE, and (d) Difference between IE and PE are illustrated, respectively. The cloud is removed by cloud detection algorithm.

Hong et al. 2010 (J. Atmos. Ocean. Tech.)